Air interface for 5G: PHY design based on pulse shaped OFDM

Malte Schellmann, Zhao Zhao, Xitao Gong, Qi Wang
Huawei European Research Center
Riesstr. 25C, 80992 Munich, Germany
Email: {malte.schellmann, erc.zhaozhao, xitao.gong, qi.wang1}@huawei.com

***Abstract*—In this paper, we present pulse shaped OFDM as an enabler for a flexible PHY design of the air interface for 5G. After introducing the waveform details and its degrees of freedom provided for the system design, we describe the suitable parameterizations to be considered for addressing the diverse requirements envisaged for future 5G systems, which are derived from the broad range of services and frequencies to be supported. Some performance results for selected scenarios underpin the superior performance of pulse shaped OFDM compared to conventional OFDM systems.**

I. Introduction

The next generation of wireless cellular networks, 5G, is expected to support a large variety of services with diverse requirements. As specified in [1], these cover extreme mobile broad band (xMBB) and novel machine type communication (MTC) services. The latter is classified into two main types, namely massive MTC (mMTC), enabling access of billions of low-cost devices anytime and anywhere, and ultra-reliable MTC (uMTC), enabling services with low latency access and with a reliability that is orders of magnitude higher than experienced in systems today. A prominent service which is expected to play a pivotal role in the context of uMTC is the vehicular to anything communication (V2X), which is supposed to provide appropriate means for enhanced traffic safety and improved traffic efficiency, ultimately enabling remotely controlled or autonomous driving. Moreover, the 5G system is expected to support a broad range of carrier frequencies, reaching from below 1 GHz up to 100 GHz. This calls for an appropriate system design responding to the distinct signal conditions and propagation properties encountered in the corresponding frequency bands. These two dimensions, i.e. the service types and carrier frequencies, form the space of the so-called '5G landscape', as defined in [2]. It is assumed that this space takes the shape of a triangle, as illustrated in Fig. 4, suggesting that for mMTC, rather the bands below 6 GHz are of highest interest, as these allow the provision of high coverage and energy efficient transmission, whereas uMTC may also use bands in higher frequencies. The entire frequency range up to 100 GHz is relevant for the xMBB service only, which may make use of any cell type deployment, such as dense small cell deployments.

The European research project METIS II [1] focuses on the design of the radio access network (RAN) for 5G, where the air interface design plays a crucial role. To appropriately address the diverse requirements opened up by the '5G landscape', more flexibility in the design of the air interface is of paramount importance. Transferring this down to the physical layer (PHY) hits on the waveform, which in today's systems is quite inflexible: In LTE, orthogonal frequency division multiplex (OFDM) is used, with a fixed configuration of PHY parameters like the subcarrier spacing, cyclic prefix (CP) length and frame structure. These parameters are usually chosen as a 'best compromise' fitting all cases that may occur during system operation. To provide flexibility also on PHY level, recent research has focused on enhancements of the OFDM waveform with filtering components [3]: Those filters enable the partitioning of a transmission band into isolated sub-bands, whose PHY parameters can then be configured individually. There are two candidate groups, namely 1) subcarrier wise filtering, comprising filter bank multi-carrier (FBMC) [4], windowed OFDM [5] and pulse shaped OFDM [6], and 2) sub-band wise filtering, where a group of subcarriers is filtered, with candidates being universal filtered (UF)-OFDM [7] and filtered OFDM [8]. FBMC in particular received a lot of attention in research during the past years [9], thanks to its favourable properties of not requiring a CP and attaining very steep filter slopes, which can facilitate an excellent isolation of the signal power in frequency domain. However, these favourable properties are 'bought' by a relaxed orthogonality (in fact, strict orthogonality holds for the real-valued signal field only), which requires a redesign of several algorithms developed for conventional OFDM systems. Due to this reason, it was hard for FBMC to get commonly accepted as a mature candidate for 5G.

In this paper, we focus on the PHY design of the air interface for 5G based on pulse shaped OFDM as the underlying waveform to cover the overall 5G landscape. We give a brief introduction into this waveform in section II, highlighting that pulse shaping provides an additional degree of freedom for the PHY design. In section III, we then describe how the waveform should be parameterized to address the requirements of the different partitions in the 5G landscape depicted in Fig. 4. The appendix provides some additional performance results of pulse shaped OFDM, highlighting the key benefits compared to CP-OFDM in two prominent scenarios for 5G applications.

II. Pulse shaped OFDM

Pulse-shaped OFDM (P-OFDM) [6] follows the idea to fully maintain the signal structure of CP-OFDM, but allowing for the use of pulse shapes other than the rectangular pulse to balance the localization of the signal power in time and frequency domain. Pulse shaping translates to a subcarrier-wise filtering as in FBMC [4], but thanks to the CP-like overhead used per symbol, complex-field orthogonality can be

maintained for the signal space, so that all schemes developed for OFDM can be reused without adaptations, including all MIMO algorithms. The complex-field orthogonality together with the reuse of the signal structure from CP-OFDM renders P-OFDM fully compatible with conventional OFDM systems.

To allow for a good spectral containment of the signal in frequency domain, the pulse shape is allowed to extend over the symbol interval T, yielding successively transmitted symbols to (partially) overlap. The overlap is characterized by the so-called overlapping factor K, which can be any rational number specifying the number of successive symbols the pulse shape spans over. For a value of K close to one, P-OFDM coincides with the well-known windowed OFDM [5]. While a value of K close to one maintains the time localization of the symbols as in CP-OFDM, chosing $K \geq 2$ creates signal properties that resemble those of an FBMC system. P-OFDM can thus be considered a hybrid solution capable of creating any compromise between a time-localized OFDM system (small K) and a frequency localized FBMC system (large K).

A. Detailed description of P-OFDM

Following the general definition of multi-carrier modulation, the time-frequency rectangular lattice is defined by the symbol interval $T = NT_s$ and the subcarrier spacing $F = (MT_s)^{-1}$, where T_s is the sampling rate of the baseband signal, N is the number of signal samples constituting one symbol interval, and M is the total number of subcarriers. For the system design of P-OFDM, we assume $N > M$, translating to an overhead in form of a cyclic prefix. This overhead can be characterized by $\vartheta = TF - 1 = N/M - 1 > 0$.

The P-OFDM transmit signal using an arbitrary transmit pulse shape $g(t)$ can be given as:

$$s(t) = \sum_{n=-\infty}^{+\infty} \sum_{m=1}^{M} a_{m,n} g(t - nT) e^{2\pi j m F t} \qquad (1)$$

where $a_{m,n}$ is the (complex-valued) information bearing symbol with sub-carrier index m and symbol index n, respectively. At the receiver, demodulation of the received signal $r(t)$ is performed based on the receive pulse shape $\gamma(t)$:

$$\hat{a}_{m,n} = \int_{-\infty}^{+\infty} r(t) \gamma(t - nT) e^{-2\pi j m F t} \qquad (2)$$

The pair of pulse shapes $g(t)$ and $\gamma(t)$ should be designed to yield an orthogonal system, thus ensuring that there is no inter-carrier and inter-symbol interference between the signals transmitted successively along the time/frequency rectangular lattice after demodulation. There are basically two different approaches for the orthogonal pulse design: The matched filter design for maximizing SNR, where $g(t) = \gamma(t)$, and the bi-orthogonal design for minimizing the interference caused by time and frequency distortions as induced by doubly dispersive channels, where $g(t) \neq \gamma(t)$.

The description of the P-OFDM signal above does not constrain the length of the pulse shape $g(t)$ to the symbol interval T as known from CP-OFDM; it only sets the orthogonality constraint as requirement. That means, the pulse shape $g(t)$ may indeed have a length of $L = KT$, with $K \geq 1$ being a rational number, yielding successively transmitted symbols to overlap up to a certain extent in time (from a fraction of the symbol duration T up to several symbol durations). Respecting the orthogonality constraint in the pulse shape design will ensure a reconstruction of the signals at the receiver without interference from preceding and succeeding symbols for any choice of K. Note that for $K \approx 1$ and using a pulse shape with smoothened edges, P-OFDM coincides with a windowed OFDM system, as described in [5].

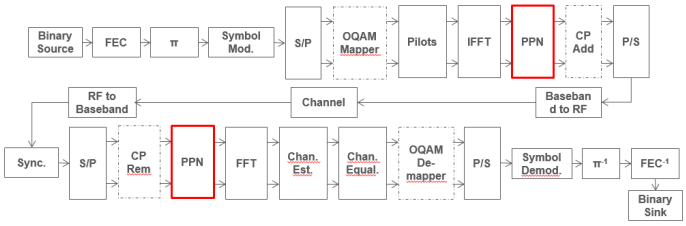

Fig. 1: P-OFDM transceiver with efficient implementation of pulse shaping by a polyphase network (PPN).

The P-OFDM transceiver for arbitrary rational overlapping factor K can be efficiently realized by a poly-phase network (PPN), which is plugged into the OFDM transmission chain after the IFFT at the transmitter and before the FFT at receiver, as shown in Fig. 1. All other algorithms for channel estimation, MIMO, etc. remain the same as for CP-OFDM. For the short pulse shape where $K \approx 1$, the PPN structure can be simplified to the 'CP', 'zero-padding'or 'windowing' operation. For a general choice of K, the PPN requires KM complex multiplications and storage for approximately $(K-1)M$ complex numbers in the register memory. For a pulse shape with $K = 4$, for example, the overall modulator complexity of P-OFDM increases only slightly by roughly 30% compared to CP-OFDM.

From the description of the P-OFDM signal given above, we can thus conclude that there are in total three degrees of freedom for the design of a multi-carrier system, which are given by the triple $(F, T, g(t))$. As the pulse shape $g(t)$ in CP-OFDM is fixed to the rectangular window, the degrees of freedom are effectively reduced. Hence, by optimizing the pulse shape $g(t)$, we therefore exploit a novel degree of freedom for the waveform design compared to CP-OFDM, enabling us to attain performance improvements in selected scenarios without altering the signal structure inherent to CP-OFDM.

B. Spectral containment

To enable flexible spectrum usage, low out-of-band (OOB) power leakage is desired. The OOB power leakage can be obtained from a frequency analysis of the transmit signal using Welch's method and characterizes the spectral containment of the transmit signal. For the comparison of P-OFDM with CP-OFDM, we consider a CP overhead of $\vartheta = 7\%$. From the power spectral density (PSD) shown in Fig. 2, we can observe that P-OFDM with an appropriately designed pulse shape filter achieves a much lower OOB power leakage than CP-OFDM does. Note that, in practice, a subband-wise low pass filtering can be adopted for CP-OFDM to shape the signal and make

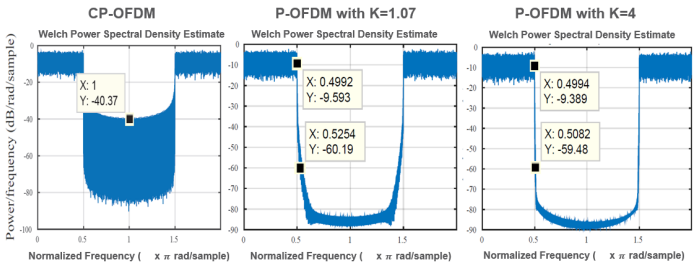

Fig. 2: PSD of CP-OFDM and P-OFDM for $\vartheta = 7\%$ overhead.

TABLE I: Required guard carriers to obtain power suppression of -50 dBc/Hz

		$K = 4$	$K = 1.07$
$\vartheta = 7\%$	Guard subcarriers	9	27
	EVM for edge subcarrier	-48.9 dB	-57.2 dB
$\vartheta = 25\%$	Guard subcarriers	7	14
	EVM for edge subcarrier	-56.8.9 dB	-55.8 dB

it fit to the spectral mask, as long as the shaping does not invoke a huge loss in error vector magnitude (EVM). Such condition holds if sufficient guard subcarriers are applied in CP-OFDM, translating to an additional overhead as compared with P-OFDM.

In the above figures, we used an LTE-typical setting of 15 KHz subcarrier spacing for 20 MHz bandwidth. To meet a desired spectral leakage of -50 dBc/Hz, the required number of guard subcarriers for P-OFDM (without any additional subband filtering) is given in Table I, where two cases for the CP overhead, $\vartheta = 7\%$ and $\vartheta = 25\%$, have been considered. It is clearly observed that the larger K and the larger the overhead ϑ, the fewer guard carriers are required thanks to an improved spectral containment of the signal. Note that the linearity of the RF unit should be considered for finally meeting the actual spectral mask requirement.

The spectral containment of the signal power enables P-OFDM to support individual PHY configurations for the sub-bands within the system bandwidth, as illustrated in Fig. 3. These individual PHY configurations also allow for the use of service-specific signaling and independently designed frame structures to be used in each of the sub-bands.

III. Air Interface PHY Design Based on P-OFDM

To respond to the large variety of requirements from the new use cases and services in 5G, a flexible air interface design supporting different PHY configurations in the same frequency band is targeted. Compared to other filtered OFDM solutions [7], [8], P-OFDM cannot only attain a favourable spectral containment of the sub-band signals, but additionally

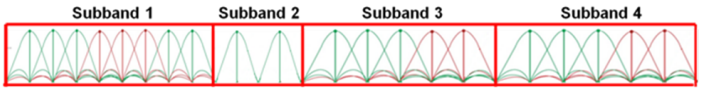

Fig. 3: Subbands with individual PHY configuration enabled by pulse shaped OFDM.

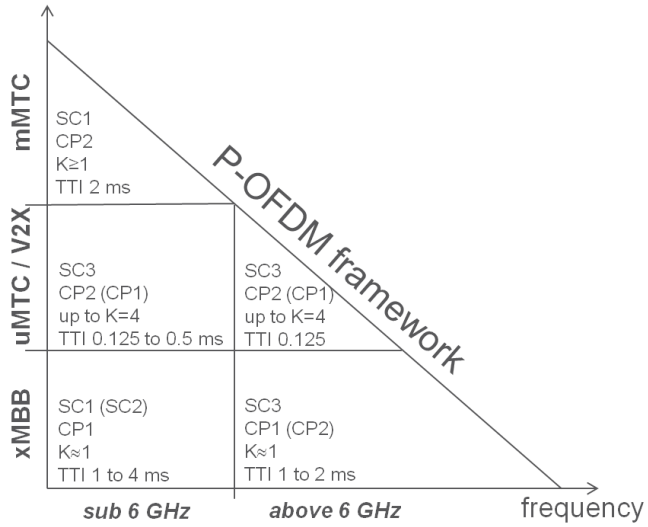

Fig. 4: Parameterizations of P-OFDM to cover the '5G landscape' of frequencies and service types.

provides an improved robustness against signal distortions like Doppler and timing misalignment. The overlapping factor K, specifying the extent of overlap between successively transmitted symbols, is a free design parameter and needs to be carefully chosen dependent on the signal conditions. For many scenarios, it is favourable to chose the overlapping factor small, letting succeeding symbols overlap by a small amount only (from 5 to 30 %) and thus yielding a time localization of the signal close to that of CP-OFDM. However, in some scenarios, in particular those building on frequency division duplex (FDD), larger overlapping factors can be afforded, enabling improved frequency localization yielding highly robust signal transmission, which could be beneficially utilized for selected uMTC applications. One of the favourable features of P-OFDM in this context is its capability to enable asynchronous multi-user access of the same frequency resources, which could be realized by OFDMA, space division multiple access (SDMA) or superposition coding. For some evaluation results on asynchronous SDMA access, refer to the Appendix.

The space of the '5G landscape', constituted by the 5G service types and targeted frequency bands can be fully covered by P-OFDM using different parameterizations, reflecting the specific PHY configurations tailored to the service needs in the targeted band. The parameterizations of P-OFDM covering the '5G landscape' are illustrated in Fig. 4. The PHY parameter sets considered for the P-OFDM based air interface PHY design are described in detail in the following:

A. Subcarrier spacing

Different subcarrier spacings are considered to allow adapting to larger subcarrier spacing in cases of high mobility or if very large bandwidth is available (like in the high frequency bands) to keep complexity to a reasonable level. The subcarrier spacing starts with 15 kHz as a basis, and is then scaled by integer multiples to allow for compatibility of the corresponding frame structures. The following three configurations are supported:

- SC1: 15 KHz (basis)
- SC2: 30 KHz
- SC3: n*15 KHz (integer multiples)

where SC1 and SC2 are supported in LTE-like deployments, and SC2 is chosen for high mobility. SC3 should be chosen for new services and use cases, like uMTC / V2X services and xMBB transmission in the high frequency bands above 6 GHz.

B. Symbol interval

As in LTE, we consider to use two different CP lengths, which can be selected according to the channel environment – the larger CP to be chosen for large delay spread channels, as experienced, for example, in Multimedia Broadcast Multicast Service (MBMS) scenario.

- CP1: 7% overhead (basis)
- CP2: 25% overhead (optional)

C. Pulse shape

a) Length: The length of the pulse shape, specified by the overlapping factor K, should be chosen depending on the desired signal conditions. In time division duplex (TDD) scenarios, strict time localization of the symbols is desired to enable fast switching between uplink (UL) and downlink (DL) transmission without long transition times induced by long symbol tails. Hence, a small value for the overlapping factor close to one ($K \approx 1$) should be the favoured choice, basically extending the symbol duration by up to half the symbol interval T at maximum: $K \in [1, 1.5]$.

In FDD or narrow band scenarios, however, the time localization of the symbols is not a strict requirement, since the UL/DL switching problem as in TDD does not exist. In this case, much larger overlap factors up to $K = 4$ could be considered, which offer the favourable support of time asynchronous multiple access to the same time/frequency resources (like SDMA or superposition coding). This property of asynchronous access is particularly beneficial in selected scenarios for MTC and V2X transmission, e.g. for low latency communication, as the time-consuming connection setup phase can then be omitted completely [6].

- $K \in [1, 1.5]$ for TDD scenarios and xMBB service
- $K \in [1, 4]$ for FDD scenarios and selected scenarios for MTC and V2X service

b) Dynamic pulse shaping: A set of useful pulse shapes, each one realizing a different distribution of the signal power in the time/frequency plane, can be provided by the system. These can be selected for particular scenarios or use cases to improve the overall quality of service. For a given frequency resource, the pulse shape may be changed dynamically according to its allocation to a service or use case. However, for longer pulse shapes (overlapping factor $K \geq 2$), reconfigurations may require some transition time, and hence changing the pulse shape is not considered to happen on a very fast time basis, but rather infrequent, yielding semi-persistent PHY configurations. For overlapping factor K close to one, this constraint is significantly relaxed, though.

D. Frame structure

Different lengths of the transmission time interval (TTI), specifying the temporal duration of a transmission frame, are considered to allow adapting to strict latency requirements as well as adjusting to larger available bandwidth in the higher frequencies. For very narrow band and MBMS services, large TTI length could be supported, which may reach up to 4 ms. For a scalable design, a minimum TTI length of 0.125 ms is considered, which is then doubled subsequently up to reaching the maximum TTI length of 4 ms. The symbol interval T should be chosen such that a TTI is always constituted of an integer number of OFDM symbols. Pilot structures should be designed such that they will also scale with the TTI length.

- Six TTI lengths: $\{0.125, 0.25, 0.5, 1, 2, 4\}$ ms

E. Uplink / Downlink design

A symmetric design for UL and DL is targeted, as this simplifies the overall system design. However, in selected scenarios, such as macro-cell deployment for wide area coverage, it may still be beneficial to resort to an UL scheme with improved peak to average power ratio (PAPR), such as DFT-spread OFDM used in today's LTE sytem, yielding better energy efficiency for battery powered devices. Such DFT precoding can also work with P-OFDM, hence an efficient pulse shaping offered by P-OFDM techniques can be applied to both DL and UL, and for low PAPR single-carrier transmissions as well.

IV. Conclusion

We have presented pulse shaped OFDM as an enabling waveform for the flexible PHY design of the air interface for 5G, and we have specified the parameterization of this waveform to address the broad requirements of the '5G landscape', constituted of the service types and frequency bands envisaged for the 5G system, as developed in [2]. In particular for the novel MTC and V2X scenarios, pulse shaped OFDM can improve the OFDM signal properties, yielding significantly higher performance compared to CP-OFDM – prominent examples are given in the appendix for the use cases of asynchronous MTC transmission and high speed trains. Thanks to the additional degree of freedom provided by pulse shaping for the system design, an air interface based on pulse shaped OFDM provides high flexibility on the PHY bedrock to respond to future requirements not yet foreseen, rendering the system design highly future-proof.

Acknowledgement

This work has been performed in the framework of the H2020 project METIS-II co-funded by the EU. The views expressed are those of the authors and do not necessarily represent the project. The consortium is not liable for any use that may be made of any of the information contained therein.

Appendix

In the following subsections, we take a look at two selected scenarios where P-OFDM can provide significantly better performance than conventional CP-OFDM. We use the LTE-based setting for CP-OFDM and assume that the P-OFDM

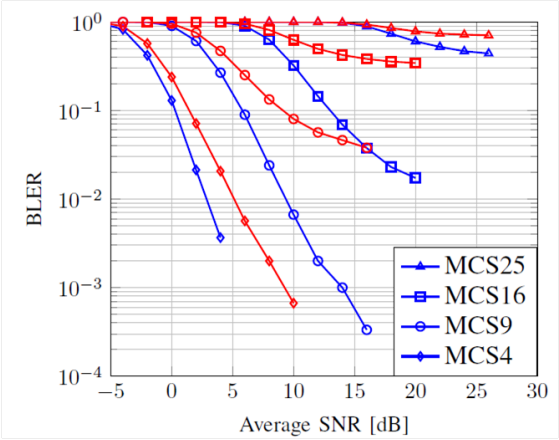

Fig. 5: BLER performance for asynchronous multi-user uplink (SDMA, ETU channels, timing offset uniformly distributed in $[0, 13]$ μs). Blue: P-OFDM, red: CP-OFDM.

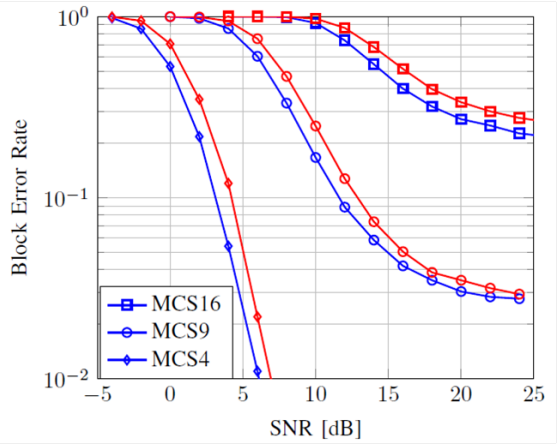

Fig. 6: BLER performance for high speed train (SISO, EVA channel, 500km/h, 15 kHz subcarrier spacing, LS channel estimation). Blue: P-OFDM, red: CP-OFDM.

scheme has the same overhead as CP-OFDM (i.e. $\vartheta = 7\%$, if not stated otherwise). Meanwhile, the same pilot structure and transceiver algorithm for equalization and channel estimation are used. Hence, we focus on the performance gain achieved solely by the optimized pulse shaping.

A. Asynchronous transmission without timing advance

We first focus on the scenario of uplink transmission where no closed-loop timing advance (TA) adjustment is applied, yielding an asynchronous transmission. Due to the radio propagation latency, the timing misalignment is present upon the arrival of the uplink signal at the BS. Assuming a cell radius of 2 km, TA misalignment is calculated according to the propagation delay of the round trip, i.e. it will lie approximately in the range of $[0, 13]$ μs.

We consider Turbo-coded block error rate (BLER) performance for two users accessing the same frequency sub-band (i.e. SDMA), which are then separated at a multi-antenna base station (BS) by using a linear minimum mean square error (MMSE) receiver. Fig. 5 depicts the results for the asynchronous transmission of two users to one BS equipped with four antennas. Since the normal CP length in OFDM of LTE systems is 4.7 μs, it cannot fully cover the time misalignment caused by the asynchronous transmission. Therefore, a performance degradation is observed for CP-OFDM for all modulation and coding schemes (MCS). P-OFDM uses an optimized pulse shape with $K = 4$, which shows significantly higher robustness to timing misalignment compared to CP-OFDM.

B. High mobility scenarios

High mobility has been recognized as a key requirement for the next generation radio technology to support a variety of new services, e.g., high speed train and V2X communication. For performance evaluation in high speed train scenario, we apply P-OFDM with a pulse shape optimzed for this high mobility with $K = 4$ and $\vartheta = 25\%$. LTE based CP-OFDM (with identical $\vartheta = 25\%$) is taken as baseline. Fig. 6 depicts the BLER performance for P-OFDM and CP-OFDM, both with least squares (LS) based channel estimation. It is shown that P-OFDM outperforms CP-OFDM thanks to its high robustness against time and frequency distortions caused by high mobility.

REFERENCES

[1] ICT-671680 METIS-II, Deliverable 1.1, "Refined scenarios and requirements, consolidated use cases, and qualitative techno-economic feasibility assessment," Jan. 2016. [Online]. Available: https://metis-ii.5g-ppp.eu/documents/deliverables/

[2] ICT-671680 METIS-II, Deliverable 4.1, "Draft air interface harmonization and user plane design," Apr. 2016. [Online]. Available: https://metis-ii.5g-ppp.eu/documents/deliverables/

[3] ICT-671660 Fantastic-5G, Deliverable 3.1, "Preliminary results for multi-service support in link solution adaptation," May 2016. [Online]. Available: http://fantastic5g.eu/

[4] B. Farhang-Boroujeny, "OFDM versus Filter Bank Multicarrier," *IEEE Signal Processing Magazine*, vol. 28, no. 3, pp. 92–112, May 2011.

[5] P. Achaichia, M. L. Bot, and P. Siohan, "Windowed OFDM versus OFDM/OQAM: A transmission capacity comparison in the HomePlug AV context," in *IEEE Intl. Symposium on Power Line Comm. and its applications*, 2011.

[6] Z. Zhao, M. Schellmann, X. Gong, Q. Wang, R. Boehnke, and Y. Guo, "Pulse shaped OFDM for 5G systems," *submitted to EURASIP Journal on Wireless Communications and Networking*, 2016. [Online]. Available: http://arxiv.org/abs/1605.03731

[7] T. Wild, F. Schaich, and Y. Chen, "5G Air Interface Design based on Universal Filtered (UF-)OFDM," in *Intl. Conference on Digital Signal Processing (DSP)*, Aug. 2014.

[8] J. Abdoli, M. Jia, and J. Ma, "Filtered OFDM: A New Waveform for Future Wiireless Systems," in *2015 IEEE 16th International Workshop on Signal Processing Advances in Wireless Communications (SPAWC)*, June 2015, pp. 66–70.

[9] ICT-317669 METIS, Deliverable 2.4, "Proposed solutions for new radio access," Feb. 2015. [Online]. Available: https://www.metis2020.com/documents/deliverables/